Geochemistry of late Mesozoic adakites from the Sulu belt, eastern China: magma genesis and implications for crustal recycling beneath continental collisional orogens

FENG GUO*, WEIMING FAN & CHAOWEN LI

Key Laboratory of Marginal Sea Geology, Guangzhou Institute of Geochemistry and South China Sea Institute
of Oceanology, Chinese Academy of Sciences, Wushan, Guangzhou, 510640, China

Abstract – Both low-Al and high-Al adakitic andesites erupted at $\sim$ 114 Ma in the Sulu collisional belt, eastern China, provide evidence for recycling of continental crust into the mantle more than 100 million years after the Triassic ($\sim$ 240 Ma) collision between the North China and Yangtze blocks. These rocks display similar normalized trace element patterns, with enrichments in large ion lithophile elements (LILE), light rare earth elements (LREE) and depletions in Nb, Ta and Ti, and have highly radiogenic Sr and non-radiogenic Nd isotopic compositions (high-Al: $^{87}Sr/^{86}Sr(i) = 0.70645$–$0.70715$ and $\varepsilon_{Nd}(t) = -20.1$ to -19.1; low-Al: $^{87}Sr/^{86}Sr(i) = 0.70593$–$0.70598$ and $\varepsilon_{Nd}(t) = -17.1$ to -15.8). The high-Al ($Al_2O_3 > 15$ %) adakitic andesites are compositionally comparable with experimental slab melts, whereas the low-Al series ($Al_2O_3 \sim 13$ %) have higher MgO, Cr and Ni, and higher Sr/Y ratios, and are compositionally comparable with slab melts hybridized by mantle peridotites. Combined major- and trace-element and Sr–Nd isotope data indicate that the two types of adakitic andesites have been derived from a LILE- and LREE-enriched eclogitic lower continental crust; in the case of the high-Al adakitic andesites, the melts underwent insignificant mantle contamination, whereas the low-Al magmas reacted with peridotites. Generation of the two types of late Mesozoic adakitic andesites favours a model of lithospheric delamination, leading to asthenospheric upwelling and extensive melting of lower continental crust, including a delaminated block, in the Sulu belt.

Keywords: geochemistry, lower continental crust, adakites, Late Mesozoic, Sulu belt.

1. Introduction

Adakites and their analogues (e.g. Archaean tonalite–trondhjemite–granodiorite rocks) are intermediate to acid rocks rich in Al_2O_3 (> 15 %) and Na_2O ($K_2O/Na_2O < 1$), with high Sr and low Y and HREE concentrations. Their origins have been attributed to high-pressure melting of basaltic protoliths, leaving garnet, pyroxene and amphibole in the residue (e.g. Defant & Drummond, 1990; Martin, 1999). Such rocks were first found in convergent plate margins and considered to be melts derived from hot and young (< 25 Ma) subducted oceanic lithosphere (Defant & Drummond, 1990). Other models for adakite generation invoke melting of older oceanic lithosphere in the course of flat subduction (Gutscher *et al.* 2000; Beate *et al.* 2001), melting along tears in subducting slabs, melting of remnant slabs in the mantle, and melting related to oblique and/or fast subduction (Defant *et al.* 2002 and references therein). In recent years, non-subduction-related adakitic magmas have been discovered in collisional zones (e.g. Chung *et al.* 2003), an intracontinental setting (Xu *et al.* 2002) and active

continental margins (e.g. some of the Andean adakites: Atherton & Petford, 1993; Petford & Atherton, 1996; Kay & Kay, 2002). Generation of the non-subduction-related adakitic magmas is commonly linked with crustal thickening and eclogitization of the lowermost crust. In summary, the prerequisite for generation of adakitic melts is that the thermal state of the lithosphere permits melting of hydrated material of generally basaltic composition, at depths corresponding to eclogite-facies (e.g. Defant & Drummond, 1990; Atherton & Petford, 1993; Martin, 1999; Xu *et al.* 2002; Petford & Gallagher, 2001; Chung *et al.* 2003). The various origins for adakites provide important constraints on crustal growth and evolution throughout the Earth's history.

Over the past decades, most studies of adakites have focused on the origin of magmas rich in Al_2O_3 (> 15 %). Adakitic magmas with low Al_2O_3 (< 15 % or even lower), however, have rarely been reported and their origins are still poorly known. Nevertheless, results from melting experiments of metabasalt at $1100\,^{\circ}C$ and 3.8 GPa (Rapp *et al.* 1999) predicted that adakitic melts hybridized by mantle peridotites would have relatively high MgO (or Mg no.), Cr and Ni concentrations and low Al_2O_3 contents as

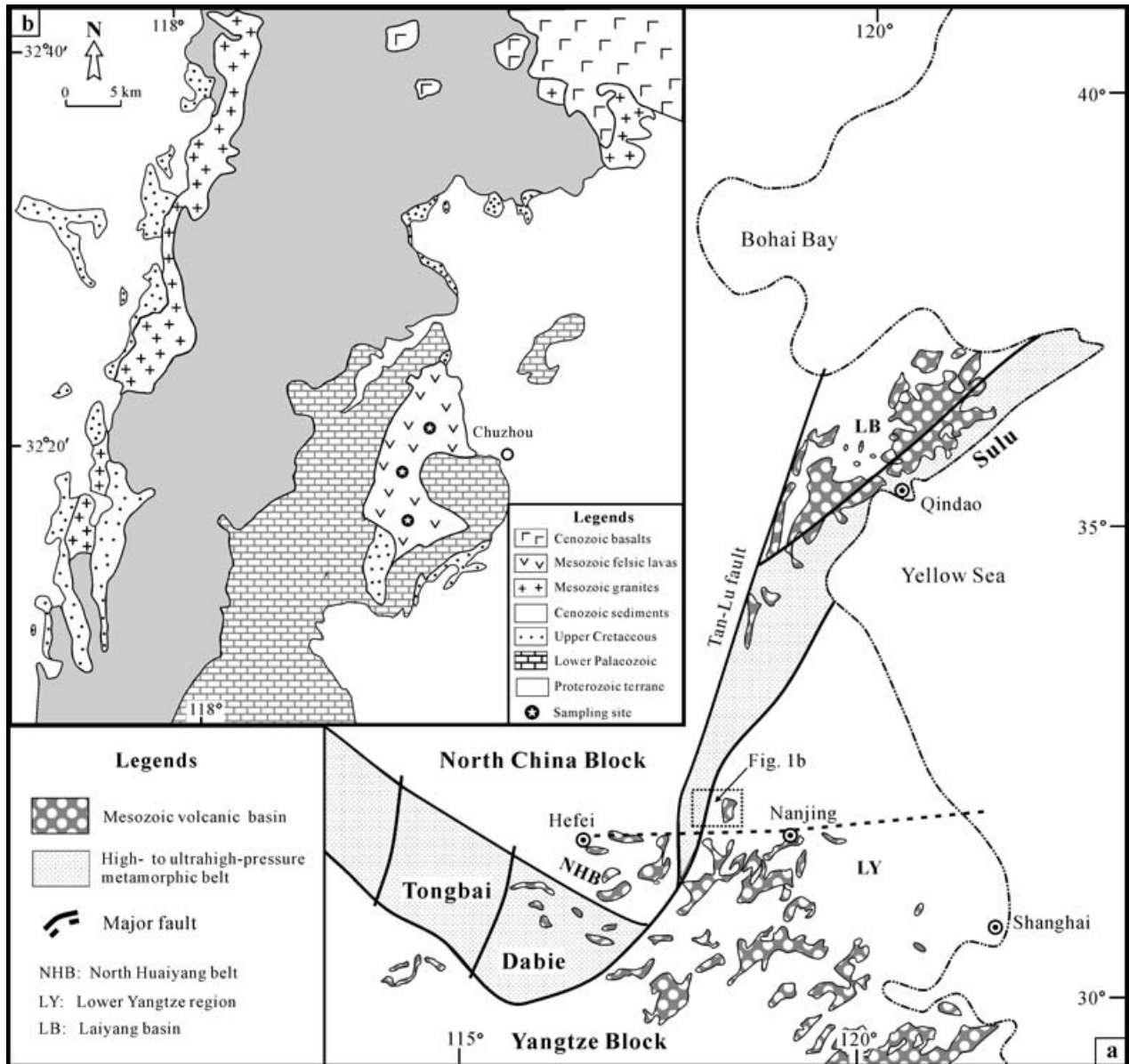* Author for correspondence: guofengt@263.net

Figure 1. A simplified map showing the distribution of HP–UHP metamorphic terranes and of late Mesozoic volcanic rocks in the Sulu belt and the adjacent regions (a), and the regional geology for Chuzhou area (b).

a result of olivine decomposition and crystallization of orthopyroxene and garnet during melt–peridotite reaction.

The Dabie-Sulu high- to ultrahigh-pressure (HP–UHP) metamorphic terrane is widely recognized as the Triassic collisional orogen between the North China and Yangtze blocks (e.g. Li *et al.* 1993; Zheng *et al.* 2002). The preservation of UHP minerals such as coesites, diamond inclusions in eclogites and metapelites, and clinopyroxene, rutile and apatite exsolutions in garnet suggest that the continental crust had been subjected to mantle depths in excess of 200 km (e.g. Xu *et al.* 1992; Jahn *et al.* 1996; Li *et al.* 1999; Ye, Ye & Cong, 2000). Along the Dabie-Sulu belt, and in the surrounding regions, are broadly distributed late Mesozoic volcanic rocks (Fig. 1a) and

voluminous granitoids (also a few adakitic intrusions, such as at Ningzhen in the Lower Yangtze region: Xu *et al.* 2002) and sporadic mafic to ultramafic intrusions (not shown). Previous studies have focused mainly on the mafic components (including basaltic lavas, mafic intrusions and dykes and lamprophyres), to investigate the contribution of subducted slabs in the formation of the enriched mantle beneath the orogen, and mantle heterogeneity under different tectonic units (e.g. Jahn *et al.* 1999; Fan *et al.* 2001, 2004; Yang & Zhou, 2001; Chen *et al.* 2001; Guo *et al.* 2004, 2005). Studies of felsic components have concentrated on the sources and magmatic evolution, and on their possible relationship with the mafic rocks (e.g. Fan *et al.* 2001, 2004; Ma *et al.* 1998; Guo *et al.* 2005; Zhao, Wang & Cao, 1997).

Given the present crustal thickness of 32–35 km (Yang, 2002), the thickened crust inferred from the UHP rocks beneath the Dabie-Sulu belt had clearly been thinned after collision. This thinning process has been poorly studied, and its role in the lithospheric evolution is still poorly constrained. Our studies of late Mesozoic volcanic rocks from the Chuzhou area in the Sulu belt uncovered a felsic suite composed of two kinds of adakitic andesites. We found that these could be clearly distinguished based on their Al_2O_3 content, with a low-Al series characterized by Al_2O_3 around 13 % (with the one exception of 20CHZ-19 that has Al_2O_3 of 15.20 %) and a high-Al series with $Al_2O_3 > 15$ %. Here we report K–Ar dating, major- and trace-element compositions and Sr–Nd isotope results of these two types of adakitic andesites. We compare these data with available data of the contemporaneous felsic volcanic rocks from the adjacent regions in order to investigate the origin of these adakites and their relationship to the crustal evolution in a collisional orogen.

2. Geological background

The North China Block and Yangtze Block are the two major continental blocks in eastern China separated by the Triassic Qinling–Dabie–Sulu collisional belt (Fig. 1a). These two blocks have undergone different crustal evolution histories. In the North China Block, the exposed lower–middle crust comprises early to late Archaean felsic and mafic granulites and tonalite–trondhjemite–granodiorites (e.g. Jahn & Zhang, 1984), with the oldest crustal rocks > 3.8 Ga (Liu *et al*. 1992). The present lowermost mafic crust is considered to be composed of metagabbro, granulite and pyroxenite xenoliths hosted in Neogene basalts (e.g. Hannuoba, Zhou *et al*. 2002; Liu *et al*. 2004). The lower–middle crust of the Yangtze Block is represented by the Kongling Group, which is composed of predominant high-grade metasediments, tonalite–trondhjemite–granodiorites and subordinate amphibolites (Gao *et al*. 1999; Ma *et al*. 2000), with the oldest crustal ages > 3.2 Ga (Qiu *et al*. 2000). By contrast, the lower–middle crust beneath the collisional orogen is still poorly constrained. Nevertheless, studies on Mesozoic I-type granitoids and metaluminous felsic volcanic rocks in this orogen suggested that the lower–middle crust comprises predominant high-grade meta-igneous protoliths with a few accumulates of basaltic/lamprophyric melts derived from an LILE- and LREE-enriched mantle (e.g. Zhao, Wang & Cao, 1997; Ma *et al*. 1998; Guo *et al*. 2005).

The Sulu belt is the eastern segment of the Triassic collisional orogen between the North China Block and Yangtze Block (e.g. Li *et al*. 1993; Zheng *et al*. 2002; Fig. 1a) and has become a significant region for studies of continental subduction, crust–mantle interaction and crustal recycling processes in continental collisional orogens. The regional geology of the area

has previously been described by Jahn *et al*. (1996), Li *et al*. (1999), Fan *et al*. (2001) and Guo *et al*. (2004, 2005). The regional tectonic evolution since early Mesozoic times can be summarized in terms of four main stages: (1) subduction of the Yangtze continental slab underneath the North China Block with peak UHP metamorphism at ∼ 240 Ma (e.g. Li *et al*. 1993; Zheng *et al*. 2002); (2) rapid exhumation of HP–UHP rocks and emplacement of alkaline complexes at 225–205 Ma, probably as a result of slab breakoff (Xu *et al*. 1999; Chen *et al*. 2003); (3) intracontinental orogenesis characterized by compressional deformation styles from 200(?) to 160 Ma, and terminated by the emplacement of peraluminous (or S-type) granitoids (Li, 1994; Zhou & Lü, 2000); (4) lithospheric extension and attenuation of the thickened lithosphere, leading to emplacement of mafic dykes and voluminous I- and A-type granitoids, mafic intrusions/dykes and the associated gold mineralization from 130 to 120 Ma (Guo *et al*. 2004; Yang & Zhou, 2001), and eruption of mafic to felsic high-K calc-alkaline magmas from 130 to 92 Ma (Fan *et al*. 2001; Guo *et al*. 2005).

The Chuzhou area is located in the southern Sulu belt, east of the Tan-Lu fault. It is bounded by the Jiashan-Xiangshui fault (F2) in the north and the Nanjing-Hefei fault in the south (Fig. 1a). The oldest exposed metamorphic basement is represented by the Zhangbaling Group, which is composed mainly of low- to medium-grade meta-igneous rocks of Neoproterozoic age (Wu *et al*. 2003; Zhou, 1995). The lower Palaeozoic marine sediments constitute the sedimentary cap, overlying the metamorphic basement and intruded by Mesozoic granitoids (Fig. 1b). The late Mesozoic volcanic sequences (termed the Huangshiba Formation) in this area crop out as parallel to subparallel layers, truncating the Proterozoic metamorphic basement and lower Palaeozoic marine sediments.

Samples were collected from a profile about 10 km west of Chuzhou city. These rocks show little trace of surface alteration. Outcrops consist predominantly of high-Al adakitic andesites and subordinate low-Al series rocks. The high-Al rocks are aphanitic to weakly porphyritic with a few phenocrysts of hornblende and plagioclase set in the groundmass of plagioclase, quartz and opaque oxides (< 0.5 mm). The low-Al lavas are porphyritic with predominant hornblende phenocrysts and minor plagioclase phenocrysts 1–3 mm in size. The groundmass is composed of fine-grained hornblende, plagioclase, quartz and opaque oxides (< 0.5 mm).

3. Analytical techniques

All samples were crushed to millimetre-scale after removal of weathered rims, handpicked under a binocular microscope and then cleaned in an ultrasonic bath with de-ionized water. These chips were then crushed to < 20 mesh in a corundum crusher. A split was ground to < 160 mesh grain size in an

Table 1. K–Ar dating results of late Mesozoic adakites in the Sulu belt, eastern China

Sample	Rock type	Weight (g)	K_2O (wt %)	^{40}Ar radiogenic (10^{-10} mol g^{-1})	% Radiogenic ^{40}Ar	^{40}K (10^{-8} mol g^{-1})	Apparent age (Ma)
20CHZ-5	High-Al adakite	0.092	3.02	4.676	86.03 %	7.491	113.7 ± 1.8
20CHZ-12	High-Al adakite	0.085	4.29	7.289	90.70 %	10.625	114.4 ± 1.8

agate ring mill for major- and trace-element analyses. Major elements were analysed at the Hubei Institute of Geology and Mineral Resources, Ministry of Land and Resources (MLR), by wavelength X-ray fluorescence spectrometry (XRF) with analytical errors ≤ 1 %.

Trace element abundances of the samples were determined using an inductively coupled plasma mass spectrometer (ICP-MS) at Guiyang Institute of Geochemistry, Chinese Academy of Sciences. About 100 mg of powder were placed in a screw-top PTFE-lined stainless steel bomb and dissolved by HF and HNO_3. The sealed bombs were placed in an electric oven and heated to 190 °C for 12 h. Before ICP-MS analysis, 1 ppm Rh solution was added as an internal standard. The analytical errors are estimated to be less than 5 % for most elements > 10 ppm and about 10 % for transition metals such as Cr, Ni, V and Sc from repetitive analyses of international standards of BHVO-1 (basalt) and AMH-1 (andesite). Duplicate runs gave < 10 % relative standard deviation for the analysed elements. Detailed description of the analytical technique was reported by Qi, Hu & Gregoire (2000).

Sr and Nd isotopic analyses were performed at the Institute of Geology and Geophysics, Chinese Academy of Sciences. Sr and Nd isotopic ratios were normalized to $^{86}Sr/^{88}Sr = 0.1194$ and $^{146}Nd/^{144}Nd = 0.7219$, respectively. Thirteen analyses of the La Jolla standard gave $^{143}Nd/^{144}Nd = 0.511862 \pm 10$, and two analyses of BCR-1 gave $^{143}Nd/^{144}Nd = 0.512626 \pm 9$. Six analyses of NBS 987 yielded $^{87}Sr/^{86}Sr = 0.710265 \pm 12$, and $^{87}Sr/^{86}Sr = 1.20032 \pm 3$ for two analyses of NBS607. Total procedure blanks are about $2–5 \times 10^{-10}$ g for Sr and less than 5×10^{-11} g for Nd. $^{87}Rb/^{86}Sr$ and $^{147}Sm/^{144}Nd$ ratios were calculated using Rb, Sr, Sm and Nd concentrations by ICP-MS analysis. $^{87}Sr/^{86}Sr(i)$ and $\varepsilon_{Nd}(t)$ were calculated using the mean K–Ar age of 114 Ma.

K–Ar dating was performed by a mass spectrum MM-1200 at Guangzhou Institute of Geochemistry, Chinese Academy of Sciences. Glassy or aphanitic samples were selected for K–Ar analysis. Rock slips were crushed to 0.2–0.9 mm grain size. Age calculation parameters used in this paper are: $^{40}K = 0.1167$ %, $K_e = 5.811 \times 10^{-11}$ a^{-1}, $K_b = 4.962 \times 10^{-10}$ a^{-1}. The analytical result for the Chinese standard ZBH-2506 is 132.32 ± 2.09 Ma (its international recommended age is 132.0 Ma). K–Ar dating, major- and trace-element compositions and Sr and Nd isotope data are listed in Tables 1 through 3.

4. Results

4.a. Eruption age of the Sulu belt adakites

The eruption ages of two samples of aphanitic high-Al adakitic andesites were determined by K–Ar dating. Samples 20CHZ-5 and 20CHZ-12 yield an apparent age of 113.7 ± 1.8 Ma and 114.4 ± 1.8 Ma, respectively, with the percentage of ^{40}Ar over 85 %. Both of them show the same apparent age within analytical errors (Table 1). Low-Al adakitic andesites occur as interbeds within the high-Al lavas, and so the low-Al rocks must also have erupted at ∼ 114 Ma, slightly before the emplacement of mafic dykes associated with late-stage lithospheric thinning in the Sulu belt (stage 4) (Guo et al. 2004; Yang & Zhou, 2001).

4.b. Major and trace elements

Felsic rocks from the Laiyang basin of the Sulu belt (Fan et al. 2001; Guo et al. 2005), the North Huaiyang belt of the northern Dabie terrane (Fan et al. 2004) and the Lower Yangtze region (Xu et al. 2002; Guo, unpub. data) (Fig. 1) are contemporaneous with the adakitic andesites of the Chuzhou area. Analyses of these additional rocks are included in our dataset for comparative purposes.

All major element contents are recalculated on a volatile-free basis. The adakitic andesites from the Chuzhou area span a SiO_2 range of 60.50–65.96 % and MgO range of 0.92–3.86 %. Compared to the high-Al adakitic andesites, the low-Al rocks generally have higher SiO_2, MgO and Mg no. (Fig. 2), higher concentrations of compatible elements such as Cr, Ni and Sc, and lower Al_2O_3, Y and HREE (Table 2). The compositions of the high-Al adakitic andesites are generally comparable with those of experimental slab melts produced at 1.0–4.0 GPa with residual assemblage of garnet + pyroxene + amphibole (e.g. Rapp & Watson, 1995), while the low-Al adakitic andesites have compositions similar to the results of experiments that simulate hybridization of slab-melts by mantle peridotites (Rapp et al. 1999; Fig. 2a, b). Except for one sample (CHZ-21), our data plot in the field defined by Cenozoic adakites and Archaean tonalite–trondhjemite–granodiorite rocks on a Y v. Sr/Y diagram (Fig. 3).

The high-Al and low-Al adakitic andesites from the Chuzhou area show only weak change in Cr and Ni despite the significant change in SiO_2 and Mg no., as might be expected if partial melting was the main
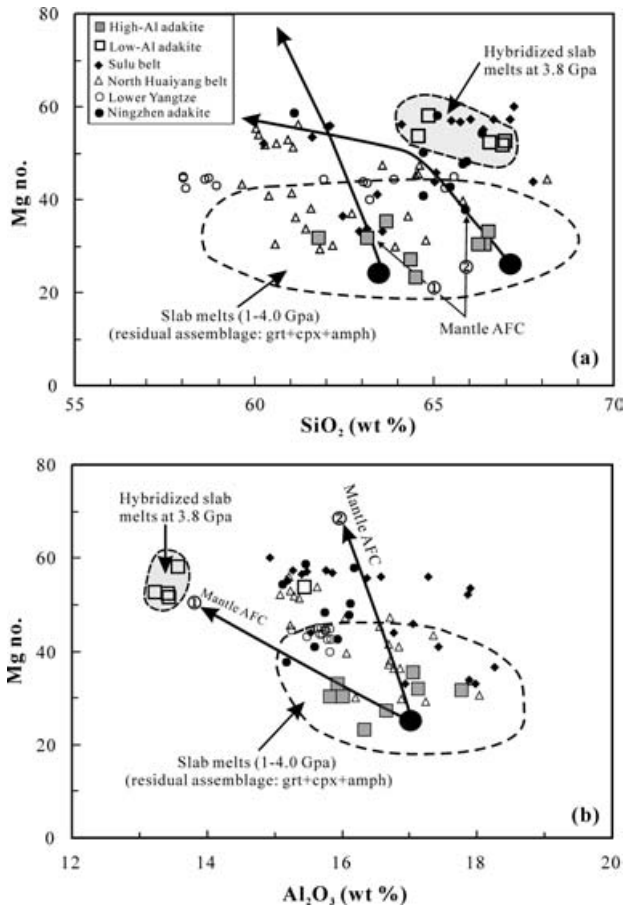
Figure 2. Mg no. v. SiO₂ (a) and Al₂O₃ (b) plots of the late Mesozoic felsic volcanic rocks from the Chuzhou area and comparison with other felsic lavas from the Dabie-Sulu belt and the Lower Yangtze region. Data sources: high-Al and low-Al adakitic andesites (this study); felsic lavas from the northern Huaiyang belt (Fan *et al*. 2004), the Sulu belt (Guo *et al*. 2005), the Lower Yangtze region (Guo, unpub. data), and the Ningzhen adakitic plutons from the Lower Yangtze (Xu *et al*. 2002); field of slab melts (Rapp & Watson, 1995) and that of hybridized slab melts (Rapp *et al*. 1999). In (a), mantle AFC curves are from Rapp *et al*. (1999, curve 1) and Stern & Kilian (1996, curve 2). In (b), two types of mantle AFC trends are responsible for Al₂O₃ variation, involving crystallization of orthopyroxene (curve 2) or garnet and orthopyroxene (curve 1). See details in text. AFC – Assimilation (coupled with) fractional crystallization.

process controlling magmatic evolution (Fig. 4a, b). Despite high SiO₂ concentrations, the low-Al adakitic andesites have the highest MgO, Mg no., Cr and Ni concentrations for felsic rocks from the Sulu belt, the northern Huaiyang belt and the Lower Yangtze region. Such features have elsewhere been interpreted as signatures of melt–mantle interaction (e.g. Kay, 1978; Kelemen, 1995; Yogodzinski *et al*. 1995; Smithies, 2000).

Both types of adakitic andesites show highly LREE- and LILE-enriched normalized trace element patterns with Nb, Ta and Ti depletions but with only negligible Eu anomalies (Fig. 5). The high-Al adakitic andesites show a range in chondrite-normalized La/Yb

(La/Yb$_{CN}$) from 13 to 22 and a Dy/Yb$_{CN}$ range from 1.25 to 1.51. Patterns for the low-Al counterparts are more fractionated with a La/Yb$_{CN}$ range from 21 to 26 and Dy/Yb$_{CN}$ from 1.52 to 1.65.

4.c. Sr–Nd isotopes

Sr and Nd isotopic data of the two types of adakitic andesites are listed in Table 3. Both adakitic andesite types have highly radiogenic Sr and non-radiogenic Nd isotopic compositions (high-Al: $^{87}Sr/^{86}Sr$ (114 Ma) = 0.70645–0.70715 and $\varepsilon_{Nd}(t) = -20.1$ to -19.1; low-Al: $^{87}Sr/^{86}Sr$(114 Ma) = 0.70593–0.70598 and $\varepsilon_{Nd}(t) = -17.1$ to -15.8), features that distinguish them from adakites created by partial melting of subducted mid-oceanic-ridge basalt (MORB) (e.g. on Cook Island: Stern & Kilian, 1996; on Adak Island: Yogodzinski *et al*. 1995; and at Cerro Pampa: Kay, Ramos & Marquez, 1993). They are also isotopically different from the contemporaneous felsic lavas and Ningzhen adakitic intrusions from the Lower Yangtze region (Fig. 6a; Xu *et al*. 2002; Guo, unpub. data), which have compositions more like those of Cenozoic adakites derived from a MORB-like slab. The Sulu belt adakitic andesites, however, have Sr and Nd isotopic compositions within the range of mafic granulite xenoliths hosted by Neogene basalts from the North China Block (e.g. at Hannuoba: Zhou *et al*. 2002; Liu *et al*. 2004), and have lower $^{87}Sr/^{86}Sr$(i) than Mesozoic mafic rocks from the Dabie-Sulu belt (Fig. 6a; Fan *et al*. 2001, 2004; Yang & Zhou, 2001; Guo *et al*. 2004, 2005). The high-Al adakitic andesites plot within the range of the Mesozoic I-type granitoids in the Sulu belt (Zhao, Wang & Cao, 1997; Zhou & Lü, 2000).

5. Discussion

In the following section, we discuss the origin of these melts (including possible protoliths and the role of melt–mantle interaction) and implications for crustal evolution beneath the collisional belt.

5.a. Possible protoliths

The compositional and isotopic differences between the two types of adakitic andesites from the Chuzhou area (Table 2, Figs 2, 3) may be attributed either to a variety of different source rocks or to variations in melting conditions, such as H₂O content, pressure, temperature and oxygen fugacity (e.g. Wolf & Wyllie, 1994; Gardien *et al*. 1995; Patiño Douce & Beard, 1995; Thompson & Connolly, 1995; Borg & Clynne, 1998; Petford & Gallagher, 2001). Sr–Nd isotopic considerations suggest that the possible sources for the adakitic andesites from the Sulu belt are: (1) an enriched lithospheric mantle sampled by basaltic lavas and lamprophyres in the Sulu belt with an $^{87}Sr/^{86}Sr$(120 Ma) from 0.7075 to 0.7095 and εNd(120 Ma) of -17 to -12

Table 2. Major and trace element compositions of late Mesozoic adakites in the Sulu belt, eastern China

| Sample Rock type	20CHZ-5 High-Al	20CHZ-8 High-Al	20CHZ-9 High-Al	20CHZ-10 High-Al	20CHZ-12 High-Al	20CHZ-20 High-Al	20CHZ-21 High-Al	20CHZ-22 High-Al	20CHZ-13 Low-Al	20CHZ-15 Low-Al	20CHZ-16 Low-Al	20CHZ-17 Low-Al	20CHZ-19 Low-Al	Experimental Hybrid slab melts (Rapp et al. 1999)
SiO_2	62.91	62.16	65.65	65.45	63.49	65.42	60.50	63.31	64.00	65.45	65.93	65.96	63.55	61.10–65.63
Al_2O_3	16.84	16.86	15.64	15.82	16.08	15.67	17.40	16.39	13.39	13.19	13.03	13.24	15.20	12.60–13.03
Fe_2O_3	3.10	4.69	2.93	3.19	5.61	3.93	5.78	4.63	4.87	4.12	4.00	4.17	3.59	
FeO	1.77	0.70	1.33	1.13	0.40	0.57	0.35	0.45	0.62	1.08	1.10	1.03	1.13	4.02–5.50
MgO	1.39	1.28	0.96	0.97	0.92	1.13	1.43	0.96	3.86	2.92	2.91	2.84	2.82	2.36–3.94
CaO	5.01	4.37	4.49	4.41	3.64	3.60	3.75	3.51	3.42	3.08	3.11	2.95	3.80	1.98–2.25
Na_2O	3.75	3.67	3.57	3.55	3.12	3.56	3.35	3.86	4.54	4.96	4.70	4.77	4.43	3.69–6.25
K_2O	2.86	3.46	3.04	3.08	4.15	3.52	4.21	4.10	2.96	2.48	2.58	2.52	2.85	3.83–6.99
MnO	0.09	0.08	0.14	0.14	0.04	0.04	0.04	0.04	0.07	0.07	0.08	0.05	0.06	0.04–0.11
TiO_2	0.66	0.75	0.70	0.70	0.61	0.58	0.64	0.72	0.67	0.67	0.67	0.71	0.65	1.98–2.19
P_2O_5	0.4	0.43	0.39	0.39	0.39	0.31	0.44	0.41	0.31	0.33	0.32	0.33	0.34	
CO_2	0.08	0.08	0.04	0.08	0.02	0.08	0.11	0.08	0.17	0.17	0.04	0.04	0.08	
H_2O+	0.79	1.13	0.76	0.75	1.15	1.19	1.58	1.16	0.72	1.11	1.18	1.02	1.09	
Total	99.65	99.66	99.64	99.66	99.62	99.6	99.58	99.62	99.6	99.63	99.65	99.63	99.59	
Mg no.	35	32	30	30	23	33	32	27	58	52	53	52	54	52–56
A/CNK	0.92	0.95	0.90	0.92	0.99	0.97	1.03	0.95	0.79	0.80	0.80	0.83	0.88	0.66–0.78
Sc	8.7	12	11	11	8.3	9.5	9.3	11	13.9	15.0	13.6	13.9	11.6	>10
V	88	115	108	111	78	77	90	98	104	109	100	101	96	
Cr	13	13	12	13	10	11	12	12	183	209	198	194	106	
Ni	5.9	5.8	5.4	5.0	4.1	7.2	5.7	19	71	87	78	75	60	
Ba	1458	1555	1706	1591	1847	1742	1907	1782	1786	1226	1227	1310	1452	1670–1861
Rb	51.9	61.9	56.0	57.9	86.6	75.1	61.2	97.4	41.5	57.1	56.6	49.7	53.3	82–98
Sr	715	816	831	831	903	891	873	859	880	934	922	974	1085	769–1471
Zr	204	200	195	196	195	217	221	239	13.9	12.4	13.4	12.1	13.0	5.8–18.2
Hf	5.99	5.94	5.60	5.55	5.45	5.94	6.17	6.54	144	150	143	139	193	246–358
Nb	9.7	10.0	9.6	9.2	8.7	9.4	9.9	10.7	4.12	4.39	4.21	3.54	5.24	
Ta	0.55	0.53	0.55	0.50	0.47	0.51	0.53	0.56	6.9	7.4	7.0	7.0	9.0	9.7–11.4
Y	17.7	18.3	16.5	16.9	17.8	15.1	22.0	15.7	0.38	0.36	0.35	0.34	0.50	
Th	4.43	4.83	4.52	4.52	5.05	5.41	5.75	5.24	5.27	5.40	5.09	5.19	6.84	1.87–2.52
U	1.03	1.12	1.15	1.18	1.17	1.22	1.19	1.36	0.92	1.71	1.54	1.67	1.65	>0.63
La	37.57	37.20	36.51	36.57	46.53	40.34	59.51	44.45	35.23	35.90	34.87	33.55	43.19	33.4–89.5
Ce	71.38	71.86	70.76	71.60	75.29	75.72	92.12	79.93	65.58	64.91	63.50	62.50	80.35	44–65
Pr	8.00	8.03	8.03	8.09	9.02	8.42	11.45	9.25	7.66	8.06	7.53	7.67	9.30	
Nd	31.72	32.38	31.08	30.93	33.55	31.35	43.37	35.35	30.06	31.27	28.55	29.58	34.08	29–42
Sm	5.39	6.09	5.33	5.21	5.60	5.15	7.53	5.72	5.37	5.37	4.92	4.84	5.90	6.9–9.7
Eu	1.79	1.82	1.74	1.81	1.89	1.76	2.30	1.94	1.75	1.77	1.55	1.66	1.66	
Gd	4.71	4.64	4.57	4.29	4.73	4.00	5.96	4.98	4.17	4.20	3.97	3.75	4.40	4.83–5.03
Tb	0.61	0.63	0.63	0.60	0.63	0.50	0.78	0.57	0.51	0.55	0.49	0.47	0.51	
Dy	3.37	3.71	3.40	3.38	3.43	3.11	4.17	3.16	2.71	2.65	2.50	2.45	2.84	2.39–4.8
Ho	0.71	0.67	0.62	0.62	0.62	0.58	0.79	0.55	0.44	0.46	0.43	0.40	0.48	>0.40
Er	2.01	1.97	1.75	1.62	1.82	1.54	2.23	1.59	1.28	1.27	1.27	1.14	1.27	0.71–2.3
Tm	0.25	0.24	0.25	0.23	0.23	0.23	0.29	0.23	0.17	0.17	0.16	0.16	0.20	
Yb	1.70	1.68	1.48	1.63	1.72	1.59	1.87	1.36	1.13	1.14	1.02	1.00	1.12	<0.5–2.0
Lu	0.26	0.25	0.22	0.23	0.24	0.23	0.27	0.22	0.18	0.17	0.17	0.13	0.16	0.08–0.4

F. GUO, W. FAN & C. LI
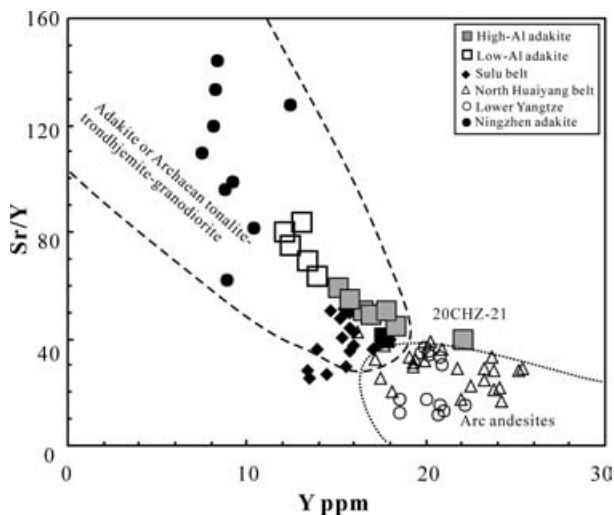
Figure 3. Y v. Sr/Y plot of late Mesozoic adakites from the Chuzhou area and comparison with other felsic rocks from adjacent regions. Data sources and symbols are same as in Figure 2.

(Fan *et al*. 2001; Yang & Zhou, 2001; Guo *et al*. 2004, 2005); (2) a lower–middle crust represented by late Mesozoic I-type granitoids and metaluminous felsic lavas that have $^{87}Sr/^{86}Sr(120\ Ma)$ from 0.7065 to 0.710 and $\varepsilon Nd(120\ Ma)$ of -22 to -17 (e.g. Zhao, Wang & Cao, 1997; Zhou & Lü, 2000); (3) the subducted Yangtze lower–middle crust, represented by the rocks of the Kongling Group, which have $^{87}Sr/^{86}Sr(120\ Ma)$ from 0.709 to 0.718 and $\varepsilon Nd(120\ Ma)$ of -47 to -25 (Gao *et al*. 1999; Ma *et al*. 2000); (4) the North China Block lower–middle crust, represented by Archaean intermediate-felsic gneisses and granulites, that have an $^{87}Sr/^{86}Sr(120\ Ma)$ ranging from 0.706 to 0.714 and $\varepsilon Nd(120\ Ma)$ of -50 to -35 (e.g. Jahn & Zhang, 1984); or (5) the lowermost mafic crust of the North China Block represented by mafic granulite xenoliths

hosted by Neogene basalts with a $^{87}Sr/^{86}Sr(120\ Ma)$ ranging from 0.7058 to 0.724 and $\varepsilon Nd(120\ Ma)$ of -29 to -9.5 (e.g. Zhou *et al*. 2002; Liu *et al*. 2004).

Late Mesozoic volcanic rocks in the North Huaiyang belt have quite radiogenic Sr $(^{87}Sr/^{86}Sr(140\ Ma) =$ 0.7086–0.7092) and non-radiogenic Nd isotopic compositions $(\varepsilon Nd(140\ Ma) = -24$ to $-19)$ and, according to Fan *et al*. (2004), they were derived from an enriched mantle source that contained relicts of subducted continental crust. As shown in Figure 6b, however, mixing between the enriched lithospheric mantle thought to be prevalent beneath the Dabie-Sulu belt, and the Yangtze (curve 4) or the North China Block (curve 3) lower–middle crust (or their melts) cannot explain the isotopic ratios in the Sulu belt adakitic andesites, especially for the low-Al series that have the least radiogenic Sr. Mixing between melts derived from the North China Block lower–middle crust and depleted mantle (Fig. 6b, curve 2) could produce the Sr–Nd isotopic compositions observed in the two types of adakitic andesites in the Sulu belt. However, although such a model is feasible for the low-Al series, it is difficult to explain the low MgO (or Mg no.), Cr and Ni concentrations (Figs 2, 4) in the high-Al adakitic andesites, which show no significant melt–mantle interaction. The fact that both the high-Al adakitic andesites and the Mesozoic I-type granitoids in the Sulu belt have similar Sr–Nd isotopic ratios to the mafic granulite xenoliths hosted by Neogene basalts from the North China Block suggests an origin for both the high-Al adakitic andesites and the I-type granites from the lower crustal mafic protoliths represented by those xenoliths. A simple and likely interpretation is that both types of adakitic andesites were derived from the lower mafic protoliths, but in the case of the low-Al series, the melts additionally interacted with depleted mantle during their ascent to the surface (curve 1 in Fig. 6b).
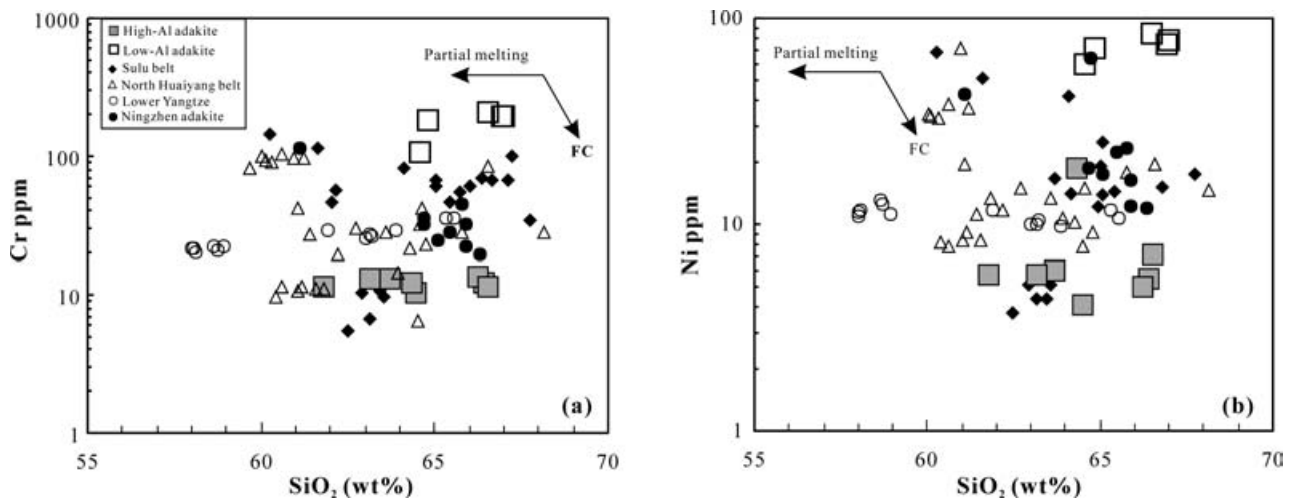

Figure 4. Cr (a) and Ni (b) v. SiO$_2$ diagrams of late Mesozoic adakites from the Chuzhou area, suggesting partial melting is the main process responsible for compositional evolution of the two types of adakitic andesites. FC – fractional crystallization. Data sources and symbols are same as in Figure 2.
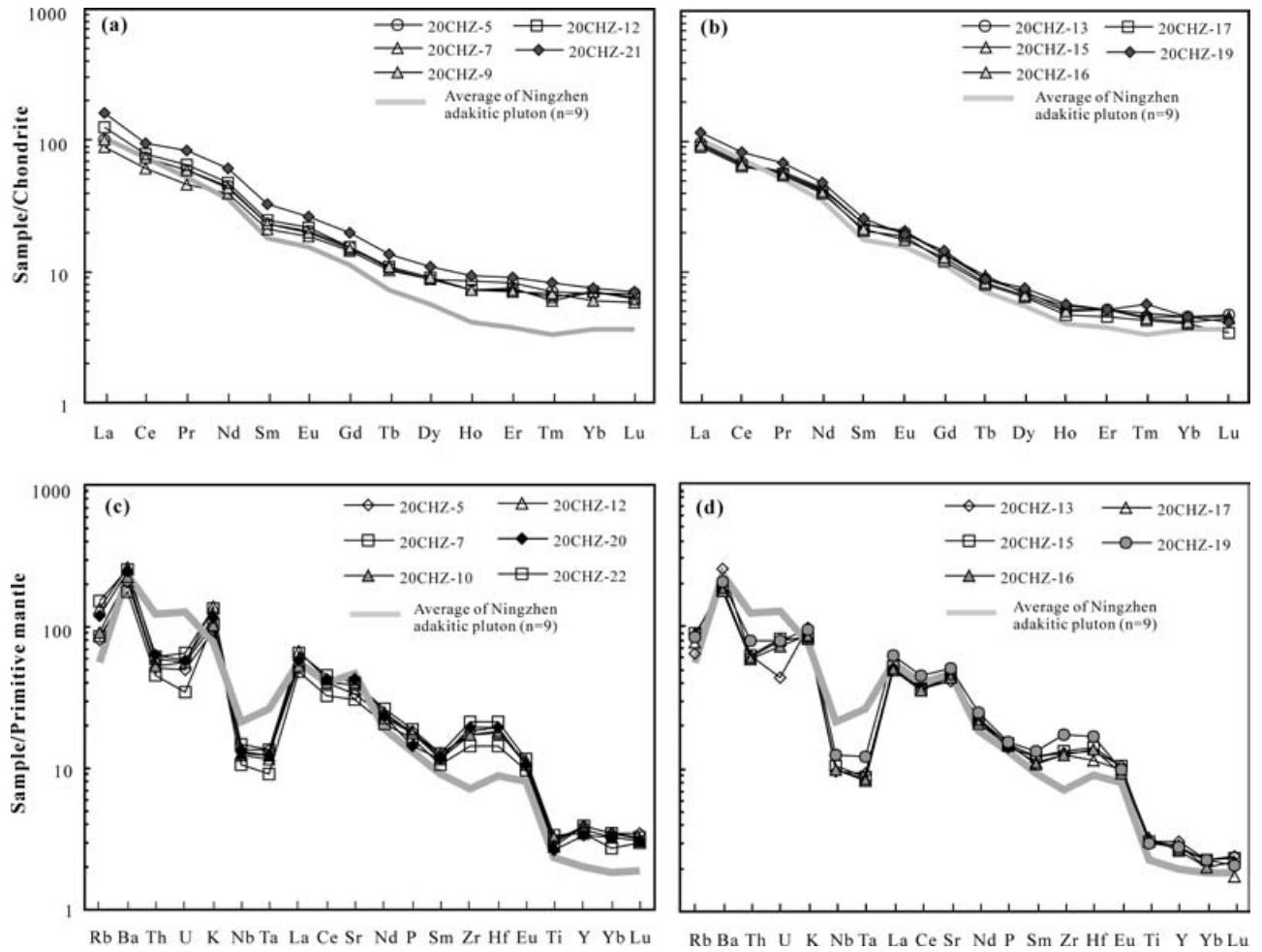
Figure 5. Chondrite-normalized REE patterns (a, b) and primitive mantle- normalized spidergrams (c, d) of late Mesozoic adakites from the Chuzhou area. The average abundances of adakitic plutons in the Lower Yangtze region (Xu *et al.* 2002) are presented for comparison. Normalized value of chondrite is from Taylor & McLennan (1985) and of primitive mantle from Sun & McDonough (1989).

5.b. Evidence for melt–mantle interaction in the low-Al adakitic andesites

The late Mesozoic Sulu belt adakitic andesites show considerable elemental similarities to modern adakites, in terms of their very low Y and Yb, and high Sr/Y and La/Yb ratios (e.g. Martin, 1999). However, the low-Al adakite series from the Sulu belt have low Al_2O_3 up to 13 % with an A/CNK range of 0.79–0.88. These features distinguish them from most modern adakites, which are rich in Al_2O_3 (e.g. > 15 %: Defant & Drummond, 1990).

Possible causes for the lower Al_2O_3 in the low-Al adakitic andesites are fractional crystallization of plagioclase, significant plagioclase residue at the time of melting or melting of a low Al_2O_3 protoliths, but the higher MgO, Mg no., Ni and Cr in these rocks are likely related to melt–peridotite reaction.

Plagioclase is the major host for CaO, Al_2O_3 and Eu and Sr in intermediate-felsic melts, so its fractionation

Table 3. Sr and Nd isotope data of late Mesozoic adakites in the Sulu belt, eastern China

| Sample	Rock type	Rb (ppm)	Sr (ppm)	$^{87}Rb/^{86}Sr$	$^{87}Sr/^{86}Sr \pm 2\sigma$	$^{87}Sr/^{86}Sr(i)$	Sm (ppm)	Nd (ppm)	$^{147}Sm/^{144}Nd$	$^{143}Nd/^{144}Nd \pm 2\sigma$	$\varepsilon_{Nd}(t)$	T_{DM} (Ga)
20CHZ-5	High-Al	52.0	715	0.2105	0.706792 ± 21	0.70645	5.39	31.72	0.1026	0.511539 ± 8	−20.1	2.22
20CHZ-8	High-Al	61.9	816	0.2196	0.707502 ± 20	0.70715	6.09	32.38	0.1136	0.511587 ± 11	−19.3	2.39
20CHZ-9	High-Al	56.0	831	0.1951	0.707460 ± 14	0.70714	5.33	31.08	0.1036	0.511584 ± 11	−19.2	2.17
20CHZ-21	High-Al	61.2	873	0.2029	0.706920 ± 20	0.70659	7.53	43.37	0.1050	0.511592 ± 11	−19.1	2.19
20CHZ-13	Low-Al	41.5	880	0.1365	0.706174 ± 18	0.70595	5.37	30.06	0.1080	0.511695 ± 10	−17.1	2.10
20CHZ-15	Low-Al	57.1	934	0.1770	0.706271 ± 20	0.70598	5.37	31.27	0.1038	0.511703 ± 12	−16.9	2.01
20CHZ-17	Low-Al	49.7	974	0.1477	0.706208 ± 20	0.70597	4.84	29.58	0.0989	0.511719 ± 12	−16.5	1.91
20CHZ-19	Low-Al	53.3	1085	0.1422	0.706161 ± 15	0.70593	5.90	34.08	0.1047	0.511761 ± 12	−15.8	1.95
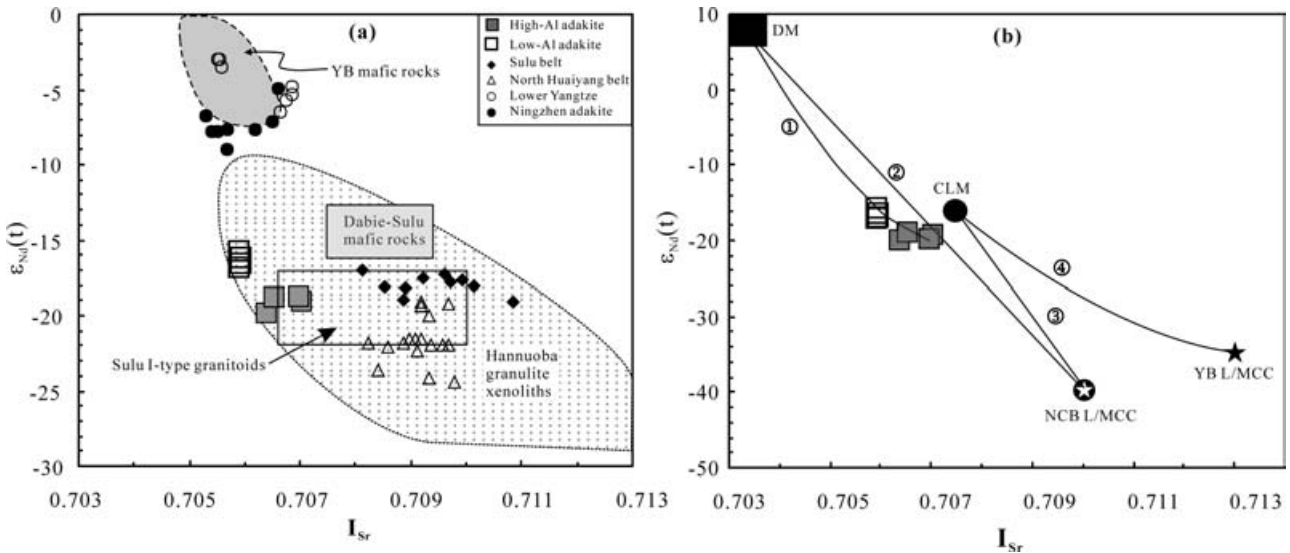
Figure 6. (a) Sr–Nd isotopic diagram of late Mesozoic adakites from the Sulu belt and (b) possible mixing models between different sources and/or melts. In (a) are compilation data for Hannuoba granulite xenoliths (Zhou *et al*. 2002; Liu *et al*. 2004), Dabie-Sulu mafic rocks (Fan *et al*. 2001; Guo *et al*. 2004; Jahn *et al*. 1999; Yang & Zhou, 2001), Sulu I-type granitoids (Zhao, Wang & Cao, 1997; Zhou & Lü, 2000), mafic rocks in the Lower Yangtze (Chen *et al*. 2001). Other data sources and symbols are same as in Figure 2. In (b), curve 1 denotes interaction between depleted mantle (DM) and high-Al melts, interaction between melts from the Archaean North China block (NCB) lower/middle continental crust (LCC/MCC) and DM on curve 2, source mixing between the enriched continental lithospheric mantle (CLM) and the North China Block LCC/MCC on curve 3, and source mixing between the enriched continental lithospheric mantle (CLM) and the Yangtze block (YB) LCC/MCC on curve 4 (Fan *et al*. 2004). Data for the Yangtze Block L/MCC (Gao *et al.* 1999; Ma *et al*. 2000) and the North China Block L/MCC (Jahn & Zhang, 1984). The bulk coefficient for Sr (K_DSr) is 0.5 and 0.8 for K_DNd. Other calculation parameters for end-member components are listed in Table 4.

will cause negative Eu and Sr anomalies in the evolved magma. Similarly, residual plagioclase at the time of melting will also lead to negative Eu and Sr anomalies. Such trace elemental features are not observed in either type of adakitic andesites from the Sulu belt, nor is it likely that a low Al_2O_3 source (e.g. garnet pyroxenites) was involved, since this would have yielded a melt of basaltic or basaltic–andesitic composition rather than intermediate-felsic composition.

We suggest that the low-Al adakite compositions are the result of mantle contamination of felsic (adakitic) melts. Kay (1978) invoked melt–peridotite interactions to explain the high Mg no., Cr and Ni concentrations in the Aleutian high-Mg adakites. Other workers (e.g. Kelemen, 1995; Yogodzinski *et al*. 1995) also place emphasis on such a process to explain similar compositional features in the magnesian andesites from other modern subduction zones. Experimental results show that reaction between slab melts and peridotites will crystallize garnet and orthopyroxene with Al_2O_3 and olivine consumption, and thus result in MgO increase and Al_2O_3 decrease in the hybridized melts (e.g. Rapp *et al*. 1999).

5.c. Implications for crustal recycling beneath collisional orogens

Geophysical surveys of the Dabie-Sulu belt, and geo-chronological studies of alkaline complexes, suggested

Table 4. Calculation parameters of end-member components for isotopic modelling in Figure 6b

Component	DM	CLM	NCB L/MCC	YB L/MCC	High-Al melt
Sr ppm	20	48	350	320	800
Nd ppm	1.2	3	24	20	32
I_{Sr}	0.703	0.7075	0.710	0.713	0.7071
$\varepsilon_{Nd}(t)$	+8	−16	−40	−35	−19

DM – depleted mantle; CLM – continental lithospheric mantle; NCB – North China block; YB – Yangtze block; L/MCC – lower/middle continental crust.

that breakoff of a subducted slab occurred shortly after the Triassic collision between the North China Block and Yangtze Block as a result of buoyancy from the convective mantle (Xu *et al*. 1999; Chen *et al*. 2003). As discussed earlier, Sr–Nd isotopic consideration suggests that reaction between melts from this remnant slab and the enriched mantle sources could not have produced the two types of adakitic andesites.

In collisional belts, the continental crust and its lithospheric mantle are vulnerable to delamination following the thickening of the lithosphere and eclogit-ization of the lowermost crust (e.g. Kay & Kay, 1993). One of the important aspects of lower crustal eclo-gitization is the presence of fluid (e.g. Leech, 2001), which accelerates the process once the crustal depth exceeds conditions required for eclogite-facies. In the Sulu belt, two factors suggest conditions favourable for
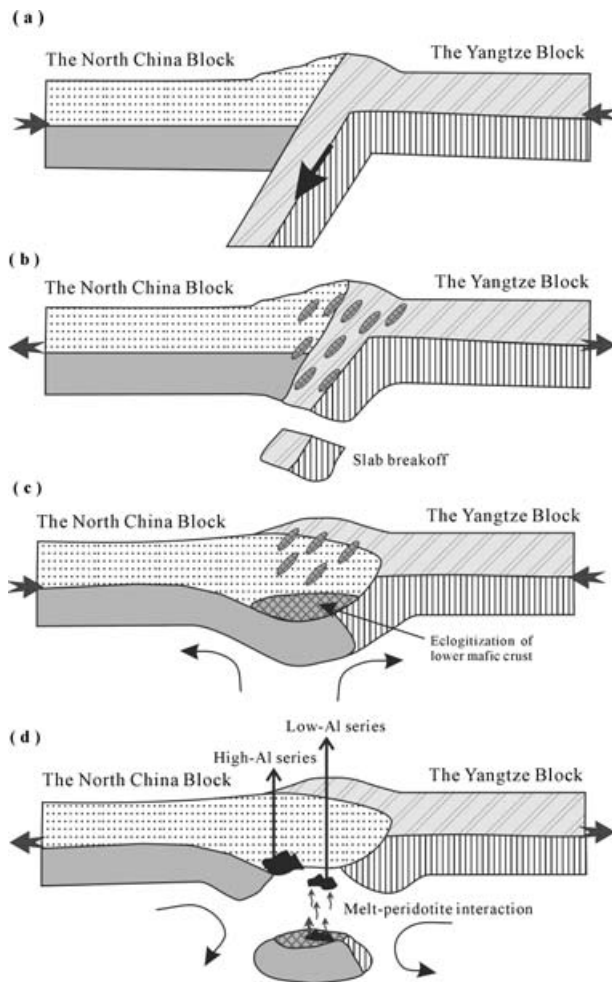
Figure 7. Cartoon showing the crustal evolution and mechanism for crustal melting beneath the Sulu belt. (a) At ∼ 240 Ma, subduction of the Yangtze continental slab into the North China Block formed a thick crust at the plate margin (e.g. Li *et al*. 1993; Zheng *et al*. 2002); (b) during the period 225–205 Ma (Chen *et al*. 2003), breakoff of the subducted slabs led to rapid exhumation of the high- to ultrahigh-pressure metamorphic terrane; (c) the following compression between the two blocks thickened the lithosphere and resulted in eclogite-facies metamorphism of the lowermost mafic crust (e.g. Li, 1994; Leech, 2001); and (d) partial delamination of the thickened lithosphere and melting of the delaminated eclogitic crustal rocks formed the primary melts for the low-Al adakitic andesites, which interacted with peridotites during the passage of the lithosphere; and delamination of the lithosphere triggered geothermal evaluation and resulted in extensive melting of newly exposed lower crustal rocks to form high-Al adakitic andesites and other metaluminous felsic intrusions and lavas along the Sulu collisional belt.

lower crustal eclogitization: (1) the existence of post-collisional magmatism at 225–205 Ma and retrogrades of the HP–UHP rocks suggest that dehydration of the subducted slab would have provided fluids/melts into the thickened crust; and (2) the subsequent intracontinental compression resulted in the further thickening of the crust. Delamination of the thickened lithosphere would have caused significant thinning of

this overthickened crust, and the enhanced geothermal elevation gradient would have heated the partially hydrated lower crustal rocks, specifically the mafic granulite now represented by mafic xenoliths in the Neogene basalts from the North China Block, sufficiently to have caused extensive melting. A scenario of Mesozoic crustal evolution and dynamics for crustal melting beneath the Sulu belt is presented in Figure 7.

In Figure 7a, the Triassic subduction (∼ 240 Ma) of a continental slab during collision between the North China Block and the Yangtze Block formed a thick crust and resulted in the peak metamorphism of the HP–UHP terrane. The subsequent breakoff of the subducted slab occurred at 225–205 Ma (Fig. 7b), which induced the rapid exhumation of the UHP metamorphic terrane and emplacement of alkaline magmas (e.g. Chen *et al*. 2003). The following intracontinental compression between the two blocks further thickened the crust and resulted in eclogite-facies metamorphism of the lowermost mafic crust (Fig. 7c). During late Mesozoic times, partial delamination of the thickened lithosphere occurred and melting of the delaminated eclogitic crust produced adakitic melts (e.g. Chazot-Prat & Girbacea, 2000). These ascended and interacted with mantle peridotites (Fig. 7d) to become the low-Al adakitic andesite series. At the same time, the delamination triggered asthenospheric upwelling, orogenic collapse and extension, and geothermal elevation of the lithosphere induced extensive melting of the newly exposed lower crustal rocks to form the high-Al adakitic andesites and other metaluminous felsic melts (e.g. I-type granitoids and felsic lavas) in the Sulu belt (Fig. 7d). We thus interpret the occurrence of both low-Al and high-Al adakitic andesites from the Sulu belt to have occurred more than 100 Ma after the Triassic collision between the North China Block and the Yangtze Block and to have involved the recycling of eclogitic crust into mantle.

6. Conclusions

Late Mesozoic (∼ 114 Ma) low-Al and high-Al adakitic andesites in the Sulu collisional belt show significant LILE and LREE enrichment, Nb–Ta depletion, and highly radiogenic Sr and non-radiogenic Nd isotopic compositions. Compositional and Sr–Nd isotopic comparison with modern subduction-related analogues suggested their derivation from an eclogitic lower continental crust with LILE and LREE enrichment. The setting and timing of this event suggests that this lower crust was partially re-hydrated continental crust, rather than the oceanic MORB-like subducted slab that typically forms the source for modern adakites. The low-Al adakitic andesites formed as part of the eclogitic lower continental crust delaminated and the melts from that sinking slab ascended through the lithospheric mantle and reacted with peridotites. The

high-Al adakitic andesite series are the result of melting of the lower portion of eclogititic crust that remained after the delamination event, and these melts never interacted with mantle peridotite. The petrogenesis of these two types of adakitic andesites in the Sulu belt suggests recycling of crustal materials into the mantle more than 100 Ma after collision between the North China Block and the Yangtze Block. Such crustal thinning and recycling processes are consistent with a model of lithospheric delamination, which triggered asthenospheric upwelling and extensive crustal melting along the Sulu collisional belt.

References

ATHERTON, M. P. & PETFORD, N. 1993. Generation of sodium-rich magmas from newly underplated basaltic crust. *Nature* **362**, 144–6.

BEATE, B., MONZIER, M., SPIKINGS, R., COTTON, J., SILVA, J., BOURDON, E. & EISSEN, J. P. 2001. Mio-Pliocene adakite generation related to flat subduction in southern Ecuador: the Quimsacocha volcanic center. *Earth and Planetary Science Letters* **192**, 561–70.

BORG, L. E. & CLYNNE, M. A. 1998. The petrogenesis of felsic calc-alkaline magmas from the southernmost Cascades, California: Origin by partial melting of basaltic lower crust. *Journal of Petrology* **39**, 1197–222.

CHAZOT-PRAT, F. & GIRBACEA, R. 2000. Partial delamination of continental mantle lithosphere, uplift-related crust-mantle decoupling, volcanism and basin formation: a new model for the Pliocene–Quaternary evolution of the southern East-Carpathians, Romania. *Tectonophysics* **327**, 83–107.

CHEN, J. F., XIE, Z., LI, H. M., ZHANG, X. D., ZHOU, T. X., PARK, Y. S., AHN, K. S., CHEN, D. G. & ZHANG, X. 2003. U–Pb zircon ages for a collision-related K-rich complex at Shidao in the Sulu ultrahigh pressure terrane, China. *Geochemical Journal* **37**, 33–46.

CHEN, J. F., YAN, J., XIE, Z., XU, X. & XING, F. M. 2001. Nd and Sr isotopic compositions of igneous rocks from the Lower Yangtze region in eastern China: constraints on sources. *Physics and Chemistry of the Earth (A)* **26**, 719–31.

CHUNG, S. L., LIU, D. Y., JI, J. Q., CHU, M. F., LEE, H. Y., WEN, D. J., LO, C. H., LEE, T. Y., QAIN, Q. & ZHANG, Q. 2003. Adakites from continental collision zones: Melting of thickened lower crust beneath southern Tibet. *Geology* **31**, 1021–4.

DEFANT, M. J. & DRUMMOND, M. S. 1990. Derivation of some modern arc magmas by melting of young subducted lithosphere. *Nature* **347**, 662–5.

DEFANT, M. J., XU, J. F., KEPEZHINSKAS, P., WANG, Q., ZHANG, Q. & XIAO, L. 2002. Adakites: some variations on a theme. *Acta Petrologica Sinica* **18**, 129–42.

FAN, W. M., GUO, F., WANG, Y. J., LIN, G. & ZHANG, M. 2001. Post-orogenic bimodal volcanism along the Sulu orogenic belt in eastern China. *Physics and Chemistry of the Earth (A)* **26**, 733–46.

FAN, W. M., GUO, F., WANG, Y. J. & ZHANG, M. 2004. Late Mesozoic volcanism in the northern Huaiyang tectono-magmatic belt, central China: partial melts from a lithospheric mantle with subducted continental crust relicts beneath the Dabie orogen? *Chemical Geology* **209**, 27–48.

GAO, S., LING, W. L., QIU, Y. M., ZHOU, L., HARTMAN, G. & SIMON, K. 1999. Contrasting geochemical and Sm-Nd isotopic compositions of Archean metasediments from the Kongling high-grade terrain of the Yangtze Craton: evidence for cratonic evolution and redistribution of REE during crustal anatexis. *Geochimica et Cosmochimica Acta* **63**, 2071–88.

GARDIEN, V., THOMPSON, A. B., GRUJIC, D. & ULUMER, P. 1995. Experimental melting of biotite–plagioclase–quartz–muscovite assemblages and implications for crustal melting. *Journal of Geophysical Research* **100**, 15581–91.

GUO, F., FAN, W. M., WANG, Y. J. & LI, C. W. 2005. Petrogenesis and tectonic implications of early Cretaceous high-K calc-alkaline volcanic rocks in the Laiyang basin of the Sulu belt, eastern China. *The Island Arc* **14**(2), 69–90.

GUO, F., FAN, W. M., WANG, Y. J. & ZHANG, M. 2004. Origin of early Cretaceous calc-alkaline lamprophyres from the Sulu orogen in eastern China: implications for enrichment processes beneath continental collisional belt. *Lithos* **78**, 291–305.

GUTSCHER, M. A., MAURY, R., EISSEN, J. P. & BOURTON, E. 2000. Can slab melting be caused by flat subduction? *Geology* **28**, 535–8.

JAHN, B. M., CORNICHET, J., CONG, B. L. & YUI, T. F. 1996. Ultrahigh-εNd eclogites from an ultrahigh-pressure metamorphic terrane of China. *Chemical Geology* **127**, 61–79.

JAHN, B. M., WU, F. Y., LO, C. H. & TSAI, C. H. 1999. Crust–mantle interaction induced by deep subduction of the continental crust: Geochemical and Sr–Nd isotopic evidence from post-collisional mafic–ultramafic intrusions of the northern Dabie complex, central China. *Chemical Geology* **157**, 119–46.

JAHN, B. M. & ZHANG, Z. Q. 1984. Archean granulite gneisses from eastern Hebei Province, China: rare earth geochemistry and tectonic implications. *Contributions to Mineralogy and Petrology* **85**, 224–43.

KAY, R. W. 1978. Aleutian magnesian andesites: melts from subducted Pacific ocean crust. *Journal of Volcanology and Geothermal Research* **4**, 117–32.

KAY, R. W. & KAY, S. M. 1993. Delamination and delamination magmatism. *Tectonophysics* **219**, 177–89.

KAY, R. W. & KAY, S. M. 2002. Andean adakites: three ways to make them. *Acta Petrologica Sinica* **18**, 303–11.

KAY, S. M., RAMOS, V. A. & MARQUEZ, M. 1993. Evidence in Cerro Pampa volcanic rocks of slab melting prior to ridge trench collision in southern South America. *Journal of Geology* **101**, 703–14.

KELEMEN, P. B. 1995. Genesis of high Mg no. andesites and the continental crust. *Contributions to Mineralogy and Petrology* **120**, 1–19.

LEECH, M. L. 2001. Arrested orogenic development: eclogitization, delamination, and tectonic collapse. *Earth and Planetary Science Letters* **185**, 149–59.

LI, S. G., JAGOUTZ, E., LO, C.-H., CHEN, Y. Z. & LI, Q. L. 1999. Sm/Nd, Rb/Sr and $^{40}Ar/^{39}Ar$ isotopic systematics of the ultrahigh-pressure metamorphic rocks in the Dabie-Sulu belt central China: A retrospective view. *International Geology Review* **41**, 1114–24.

LI, S. G., XIAO, Y. L., LIOU, D. L., CHEN, Y. Z., GE, N. J., ZHANG, Z. Q., SUN, S. S., CONG, B. L., ZHANG, R. Y., HART, S. R. & WANG, S. S. 1993. Collision of the North China and Yangtze blocks and formation of coesite-bearing eclogites: timing and process. *Chemical Geology* **109**, 89–111.

LI, Z. X. 1994. Collision between the North and South China Blocks: a crustal-detachment model for suturing in the region east of the Tanlu Fault. *Geology* **22**, 739–42.

LIU, D. Y., NUTMAN, A. P., COMPSTON, W., WU, J. S. & SHEN, Q. H., 1992. Remnants of 3800 Ma crust in the Chinese part of the Sino-Korean craton. *Geology* **20**, 339–42.

LIU, Y. S., GAO, S., YUAN, H. L., ZHOU, L., LIU, X. M., WANG, X. C., HU, Z. C. & WANG, L. S. 2004. U–Pb zircon ages and Nd, Sr, and Pb isotopes of lower crustal xenoliths from North China Craton: insights on evolution of lower continental crust. *Chemical Geology* **211**, 87–109.

MA, C. Q., EHLERS, C., XU, C. H., LI, Z. C. & YANG, K. G. 2000. The roots of the Dabieshan ultrahigh-pressure metamorphic terrane: constraints from geochemistry and Nd–Sr isotope systematics. *Precambrian Research* **102**, 279–301.

MA, C. Q., LI, Z. C., EHLERS, C., YANG, K. G. & WANG, R. J. 1998. A post-collisional magmatic plumbing system: Mesozoic granitoid plutons from the Dabieshan high-pressure and ultrahigh-pressure metamorphic zone, east-central China. *Lithos* **45**, 431–56.

MARTIN, H. 1999. Adakitic magmas: modern analogues of Archaean granitoids. *Lithos* **46**, 411–29.

PATIÑO DOUCE, A. E. & BEARD, J. S. 1995. Dehydration-melting of biotite gneiss and quartz amphibolite from 3 to 15 kbar. *Journal of Petrology* **36**, 707–38.

PETFORD, N. & ATHERTON, M. P. 1996. Na-rich partial melts from newly underplated basaltic crust: the Cordillera Blanca Batholith, Peru. *Journal of Petrology* **37**, 1491–521.

PETFORD, N. & GALLAGHER, K. 2001. Partial melting of mafic (amphibolitic) lower crust by periodic influx of basaltic magma. *Earth and Planetary Science Letters* **193**, 483–99.

QI, L., HU, J. & GREGOIRE, D. C. 2000. Determination of trace elements in granites by inductively coupled plasma mass spectrometry. *Talanta* **51**, 507–13.

QIU, Y. M., GAO, S., McNAUGHTON, N. J., GROVES, D. I. & LING, W. L. 2000. First evidence of >3.2 Ga continental crust in the Yangtze Craton of south China and its implications for Archean crustal evolution and Phanerozoic tectonics. *Geology* **28**, 11–14.

RAPP, R. P., SHIMIZU, N., NORMAN, M. D. & APPLEGATE, G. S. 1999. Reaction between slab-derived melts and peridotite in the mantle wedge: experimental constraints at 3.8 Gpa. *Chemical Geology* **160**, 335–56.

RAPP, R. P. & WATSON, E. B. 1995. Dehydration melting of metabasalt at 8–32 kbar: Implications for continental growth and crust-mantle recycling. *Journal of Petrology* **36**, 891–931.

SMITHIES, R. H. 2000. The Archaean tonalite–trondhjemite–granodiorite (TTG) series is not analogue of Cenozoic adakites. *Earth and Planetary Science Letters* **182**, 115–25.

STERN, C. R. & KILIAN, R. 1996. Role of the subducted slab, mantle wedge and continental crust in the generation of adakites from the Austral volcanic zone. *Contributions to Mineralogy and Petrology* **123**, 263–81.

SUN, S.-S. & McDONOUGH, W. F. 1989. Chemical and isotopic systematics of oceanic basalts: implications for mantle composition and processes. In *Magmatism in the Ocean Basins* (eds A. D. Saunders and M. J. Norry), pp. 313–45. Geological Society of London, Special Publication no. 42.

TAYLOR, S. R. & McLENNAN, S. M. 1985. *The continental crust: Its composition and evolution.* Oxford: Blackwell Press, 312 pp.

THOMPSON, A. B. & CONNOLLY, A. D. 1995. Melting of the continental crust: some thermal and petrological constraints on anatexis in continental collision zones and other tectonic settings. *Journal of Geophysical Research* **100**, 15565–79.

WOLF, M. B. & WYLLIE, J. P. 1994. Dehydration-melting of amphibolite at 10 kbar: the effects of temperature and time. *Contributions to Mineralogy and Petrology* **115**, 369–83.

WU, G., MA, L., CHEN, H. & XU, K. 2003. Tectonic evolution of the Su-Wan block, creation of the Su-Lu orogen and orogenesis-coupled basin developing. *Geotectonica et Metallogenia* **27**, 337–53 (in Chinese with English abstract).

XU, S., OKAY, A. I., ŞENGÖR, A. M. C., SU, W., LIU, Y. & JIANG, L. 1992. Diamond from Dabie Shan eclogites and its implication for tectonic setting. *Science* **256**, 80–2.

XU, J. F., SHINJO, R., DEFANT, M. J., WANG, Q. & RAPP, R. P. 2002. Origin of Mesozoic adakitic intrusive rocks in the Ningzhen area of east China: Partial melting of delaminated lower continental crust? *Geology* **30**, 1111–14.

XU, P. F., SUN, R. M., LIU, F. T., WANG, Q. C. & CONG, B. L. 1999. The subduction and slab breakoff between the South China block and North China block: evidence from the seismological chromatography. *Chinese Science Bulletin* **44**, 1658–61.

YANG, J. H. & ZHOU, X. H. 2001. Rb–Sr, Sm–Nd and Pb isotope systematics of pyrite: implications for the age and genesis of lode gold deposits. *Geology* **29**, 711–14.

YANG, W. C. 2002. Geophysical profiling across the Sulu ultra-high-pressure metamorphic belt, eastern China. *Tectonophysics* **354**, 277–88.

YE, K., YE, D. N. & CONG, B. L. 2000. The possible subduction of continental material to depths greater than 200 km. *Nature* **407**, 734–6.

YOGODZINSKI, G. M., KAY, R. W., VOLYNETS, O. N., KOLOSKOV, A. V. & KAY, S. M. 1995. Magnesian andesite in the western Aleutian Komandorsky region: implications for slab melting and processes in the mantle wedge. *Geological Society of America Bulletin* **107**, 505–19.

ZHAO, G., WANG, D. & CAO, Q. 1997. Geochemical features and petrogenesis of Laoshan Granite in east Shandong Province. *Geological Journal of China Universities* **3**, 1–15 (in Chinese with English abstract).

ZHENG, Y. F., WANG, Z. R., LI, S. G. & ZHAO, Z. F. 2002. Oxygen isotope equilibrium between eclogite minerals and its constraints on mineral Sm–Nd chronometer. *Geochimica et Cosmochimica Acta* **66**, 625–34.

ZHOU, J. Y. 1995. The tectonic evolution and dynamics of Zhangbaling region in Anhui province. *Volcanology and Mineral Resources* **16**(4), 17–24 (in Chinese with English abstract).

ZHOU, T. H. & LÜ, G. X. 2000. Tectonics, granitoids and Mesozoic gold deposits in East Shandong, China. *Ore Geology Reviews* **16**, 71–90.

ZHOU, X. H., SUN, M., ZHANG, G. H. & CHEN, S. H. 2002. Continental crust and lithospheric mantle interaction beneath North China: isotopic evidence from granulite xenoliths in Hannuoba, Sino-Korean craton. *Lithos* **62**, 111–24.